PHILOSOPHICAL TRANSACTIONS OF THE ROYAL SOCIETY A MATHEMATICAL, PHYSICAL & ENGINEERING SCIENCES

# Interactional Effects between Adsorbates on Metal Single-Crystals [and Discussion]

J. T. Yates, M. Trenary, K. J. Uram, H. Metiu, F. Bozso, R. M. Martin, C. Hanrahan, J. Arias and S. Holloway

*Phil. Trans. R. Soc. Lond. A* 1986 **318**, 101-115
doi: 10.1098/rsta.1986.0063

*Phil. Trans. R. Soc. Lond.* A **318**, 101–115 (1986) [ 101 ]
*Printed in Great Britain*

# Interactional effects between adsorbates on metal single-crystals

By J. T. Yates[1], Jr, M. Trenary[1]†, K. J. Uram[1], H. Metiu[2], F. Bozso[2]‡, R. M. Martin[2], C. Hanrahan[2] and J. Arias[2]

[1]*Surface Science Center, Department of Chemistry, University of Pittsburgh, Pittsburgh, Pennsylvania* 15260, *U.S.A.*

[2]*Department of Chemistry, University of California, Santa Barbara, California* 93106, *U.S.A.*

The interactions between CO species chemisorbed on Ni(111) and the interactions between CO and S on S-poisoned Ni(111) have been studied by using infrared reflection–absorption spectroscopy. For CO chemisorption on the clean surface, evidence for long-range chemical interactions is presented in which donor–acceptor effects prevail in determining CO hybridization states. For CO chemisorption on S-poisoned Ni(111), evidence for the influence of local electrostatic effects in the vicinity of the S atom is presented. Slightly longer range S···CO interactions also occur, removing the CO chemisorption ability of next-neighbour Ni sites to S. These two interaction mechanisms extend over about six Ni atom neighbours to S. Surface Penning ionization electron spectroscopy has been used to probe the filled molecular orbitals of chemisorbed CO on Ni(111), and direct evidence for the involvement in chemisorption of the CO $2\pi^*$ orbitals is found, both on the clean Ni(111) surface and on K + Ni(111).

## 1. Introduction

Modern surface-spectroscopic methods, applied to the study of chemisorbed species on single-crystal surfaces, can give detailed information about the interactions that occur between adsorbates. An issue of importance in this area is the spatial range of these interaction effects.

Chemical effects between adsorbates may be divided into two general categories: local electrostatic effects, and longer range unscreened electronic perturbations that extend across the surface. These effects have been examined theoretically by Feibelman & Hamann (1984, 1985) and by Norskov *et al.* (1984) for electronegative or electropositive impurity atoms on metals interacting with molecular adsorbates such as CO. The concepts developed in these papers relate to catalytic poisoning and promotion by impurity surface species.

Figure 1 shows the theoretical result obtained by Feibelman & Hamann (1984) for the variation of the total valence charge density with distance across and above a Rh(001) surface, containing impurity S atoms located in a $(3 \times 1)$ adlayer at fourfold hollow sites. In figure 1*a*, the electron charge density contours are plotted for the surface along a diagonal plane cut through the S atom, and through neighbour and next-neighbour Rh atoms (see the rectangular field in the inset diagram in the upper right corner). In figure 1*b*, the perturbed electron density due to S adsorption is compared with the original electron density map for the clean surface. It is clear from this figure that the perturbing electrostatic effect of the S impurity atom is screened out beyond the nearest neighbour Rh atom to S. This screening is complete at the

† Present address: Department of Chemistry, University of Illinois at Chicago, Chicago, Illinois 60680, U.S.A.
‡ Present address: I.B.M. Research Laboratories, Yorktown Heights, New York 10598, U.S.A.

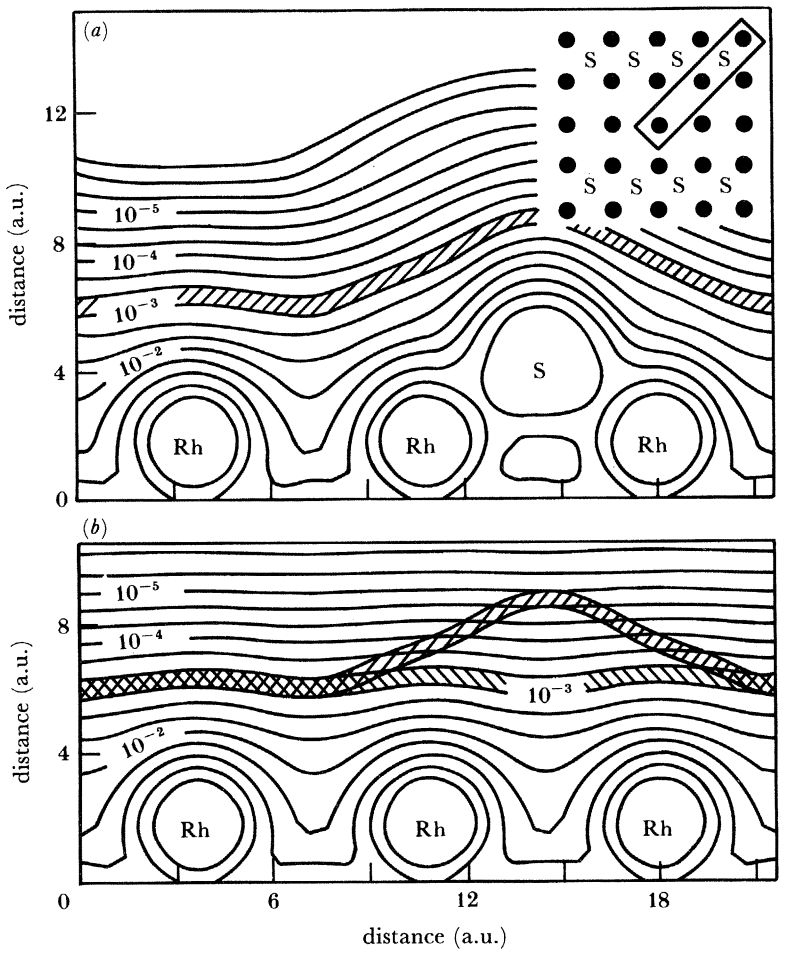


FIGURE 1. (*a*) Valence charge densities for S(3 × 1) on Rh(001). The density changes by a factor of $10^{\frac{1}{3}}\, a_B^{-3}$ $eV^{-1}$ from one contour to the next. (*b*) Comparison of valence charge density for S(3 × 1) and clean Rh(001). 1 a.u. (length) = $0.529177 \times 10^{-10}$ m.

point where the cross-hatched electron density contour region selected for illustration merges into that of the unperturbed metal. Thus, in this system, all electrostatic effects due to electronegative S must occur at Rh atoms directly adjacent to the S atom.

In contrast to this local electrostatic behaviour, chemical effects may also occur because of perturbations in the local density of states (l.d.o.s), which lie within a small energy bandwidth near the Fermi edge, $E_F$. For a $\pm 0.2$ eV bandwidth centred at $E_F$, the calculation yields a contour plot shown in figure 2*a*, for the same adsorbate S geometry as in figure 1. In figure 2*b*, a comparison is made with the l.d.o.s. for the unperturbed Rh(001) surface. The effect of S on the Rh surface is widespread in this case, causing a reduction in the l.d.o.s. over a wide lateral range. This reduction means that the surface can respond less favourably (i.e. with less lowering of energy) to an adsorbate. The l.d.o.s. is an unscreened quantity, and perturbations of it due to impurity adsorbates are long range in their lateral extent.

In this paper experimental evidence for both types of interactional effects in adlayers on a Ni(111) single-crystal is presented.

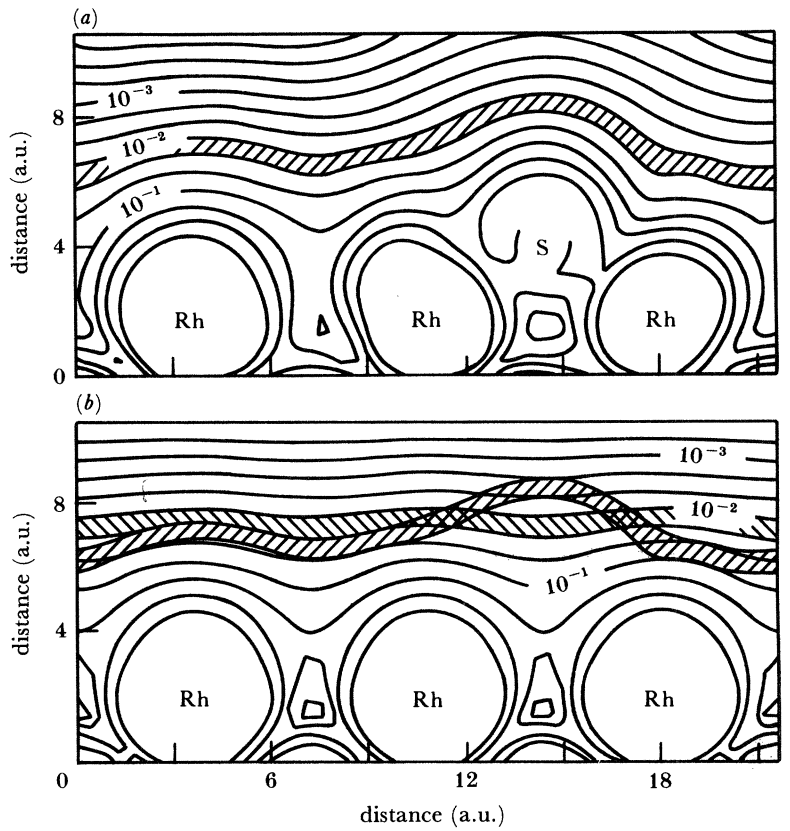


FIGURE 2. (*a*) Fermi-level local density of states for S(3 × 1) on Rh(001). The Fermi-level l.d.o.s. changes by a factor of $10^{\frac{1}{3}} a_B^{-3}$ $eV^{-1}$ from one contour to the next. (*b*) Comparison of Fermi-level l.d.o.s. for S(3 × 1) and clean Rh(001).

## 2. EXPERIMENTAL

### (*a*) *Infrared reflection–absorption apparatus* (Trenary *et al.* 1985)

The three-level ultra-high vacuum apparatus (base pressure = $6 \times 10^{-9}$ N $m^{-2}$) is shown in figure 3. Level 3 is equipped with a hemispherical electron energy analyser for X-ray photoelectron spectroscopy (X.p.s) and Auger electron spectroscopy (A.e.s.) work, a collimated molecular beam doser for gas adsorption, and a quadrupole mass spectrometer. Level 2 contains a display low-energy electron diffraction (l.e.e.d.) apparatus and a sputter gun for $Ar^+$ crystal cleaning. Level 1 is a small-volume reflection i.r. cell, which may be operated at high gas pressures if necessary. It contains $CaF_2$ windows, and may be isolated by means of a metal-sealed gate valve. The Ni(111) single crystal can be cooled to 80 K. It can be rotated 360° about the vertical axis by using a two-stage differentially pumped rotary seal. Vertical translation of the crystal through 0.7 m is possible by using a metal bellows. To intersect all of the incident i.r. radiation, 17.5 mm diameter Ni(111) crystals were used. The i.r. radiation strikes the crystal at an incidence angle of about 86°, as shown in figure 4.

Infrared measurements were made by using a purged double-beam ratio-recording grating instrument, equipped with an external optical system shown in figure 4. Integration of data for 4 s $cm^{-1}$ gave a noise level of $2 \times 10^{-4}$ absorbance units at a resolution of 6.8 $cm^{-1}$.

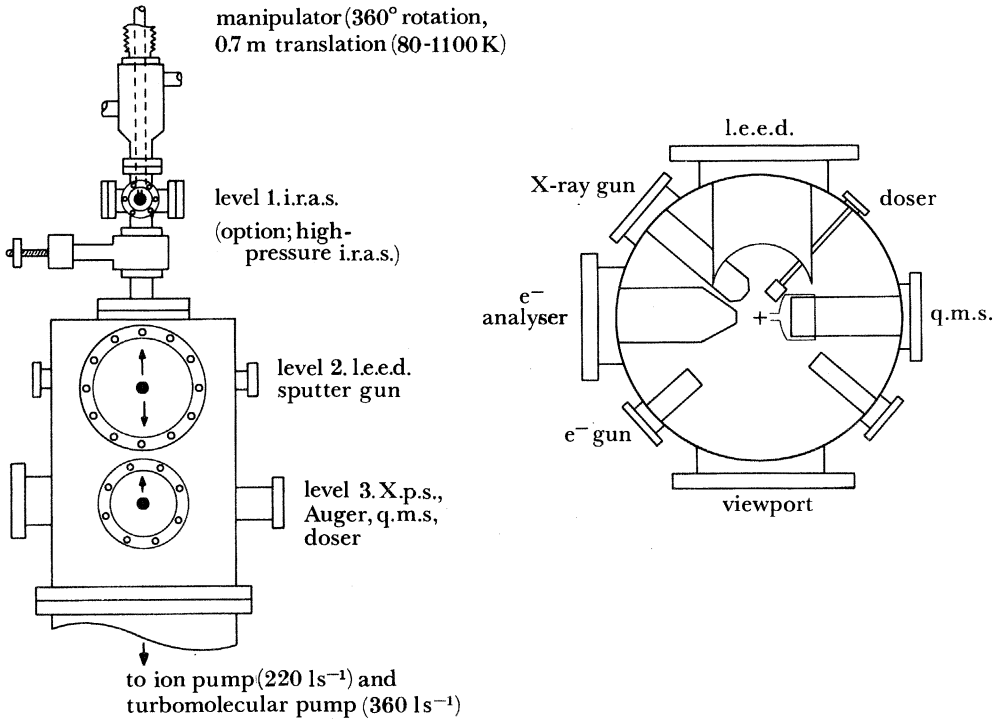


FIGURE 3. Ultra-high vacuum chamber for infrared reflection absorption spectroscopy (i.r.a.s.). At level 1, the i.r.a.s. cell may be separately isolated and pressurized.

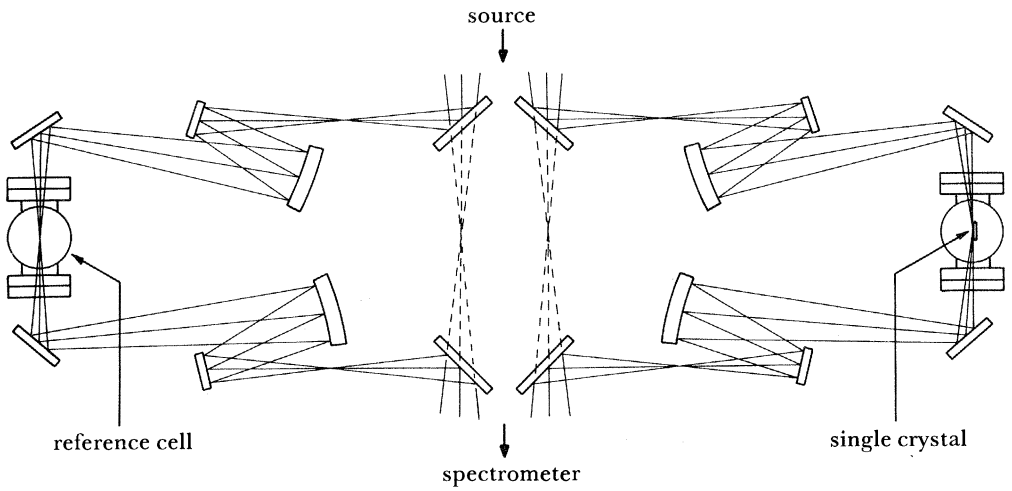


FIGURE 4. Optical system for i.r. reflection absorption studies.

The clean crystal could be covered with S by using $H_2S$, followed by annealing. For thermal desorption spectroscopy (t.d.s.) measurements, the back side of the crystal was blocked in this manner by S adsorption. All CO admitted at high pressure to the crystal at level 1 was purified by storage at 77 K.

### (*b*) *Surface Penning ionization electron spectrometer* (Bozso *et al.* 1983)

This ultra-high vacuum apparatus permitted a molecular beam of metastable $2^1S$ He atoms (20.6 eV) to impinge on a Ni(111) single crystal. The electrons ejected from the surface were

energy analysed by a hemispherical grid retarding-field analyser, equipped with a pair of 40 mm diameter microchannel electron multiplier plates behind the grid system.

## 3. Results

### (*a*) CO *adsorption on clean* Ni(111) *by infrared studies*

Figure 5 shows the correlation between i.r. spectra and the $c(4\times2)$ and $(\frac{1}{2}\sqrt{7}\times\frac{1}{2}\sqrt{7})$ R 19.1° overlayer structures for CO chemisorbed on Ni(111). No distinct l.e.e.d. pattern was observed for adsorption of CO at 80 K. Upon annealing a disordered saturated CO layer to 240 K, the $(\frac{1}{2}\sqrt{7}\times\frac{1}{2}\sqrt{7})$ R 19.1° full coverage pattern ($\theta_{CO} = 0.57$ CO/Ni) develops, and both terminal (2055 $cm^{-1}$) and bridged CO (1925 $cm^{-1}$) i.r. bands sharpen. This full coverage overlayer corresponds to one 'on-top' CO for three bridged CO species (Conrad *et al.* 1976; Campuzano & Greenler 1979; Netzer & Madey 1982).

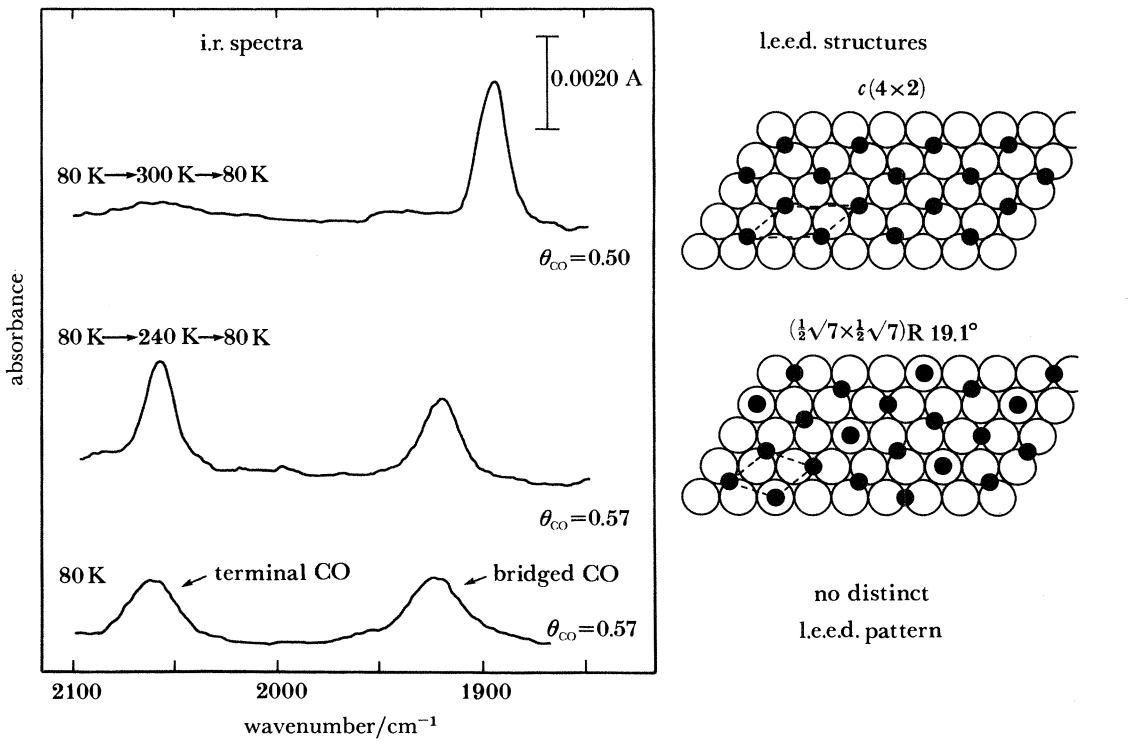


Figure 5. CO adsorption site distribution for various annealing treatments of Ni(111) + CO.

Further brief annealing in vacuum to 300 K causes the 'on-top' CO (2055 $cm^{-1}$) to desorb while the 1925 $cm^{-1}$ bridged CO band shifts to 1896 $cm^{-1}$. The corresponding l.e.e.d. pattern converts to a $c(4\times2)$ structure, corresponding to a coverage $\theta_{CO} = 0.5$ for CO/Ni. The i.r. data show that the $c(4\times2)$ structure exclusively occupies two-fold bridge sites, in agreement with previous studies (Bertolini *et al.* 1977; Erley *et al.* 1979; Bertolini & Tardy 1981; Campuzano & Greenler 1979).

Figure 6 shows a plot of the i.r. frequency for bridged CO adsorbed at 80 K as a function of surface coverage, measured by t.d.s. A linear coverage dependence of bridged CO frequency is observed up to $\theta_{CO} = 0.4$ CO/Ni, near the onset of development of the first terminal

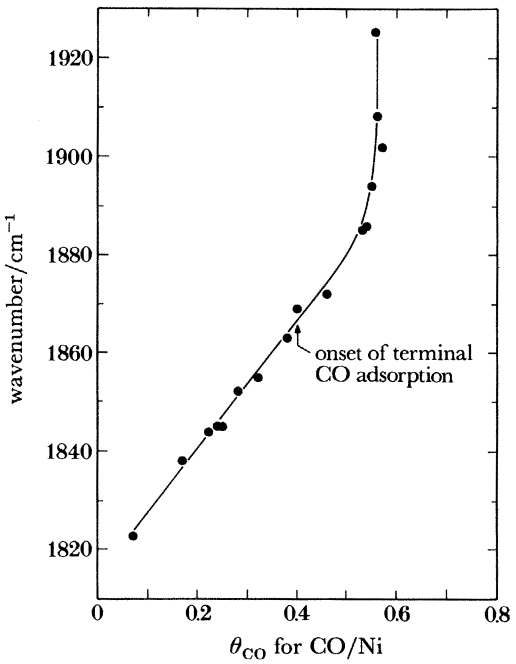


FIGURE 6. Frequency-dependence of bridged CO on Ni(111) as a function of measured (t.d.s) coverages at 80 K.

CO species. At this point, the frequency of bridged CO makes an abrupt increase of *ca.* 50–60 cm$^{-1}$ for the final CO coverage increment where terminal CO is being formed. As shown in figure 7, both bridged CO and terminal CO exhibit significant frequency shifts in the region of high CO coverage.

### (*b*) CO *adsorption on* S/Ni(111)

#### (i) *Infrared studies*

Controlled coverage of S on Ni(111) could be produced by $H_2S$ adsorption followed by annealing at 670 K to remove hydrogen. By correlation of l.e.e.d. pattern development for S overlayers with A.e.s. and $H_2$ t.d.s. measurements (Trenary *et al.* 1985) it was possible to establish a calibration curve of S(152)/Ni(102) A.e.s. peak-to-peak intensities as a function of the absolute S coverage (S atoms per square metre) with an accuracy of about $\pm 25\%$.

CO was chemisorbed at 300 K on S/Ni(111) at various S coverages by using the high-pressure i.r. cell; in this manner at high CO pressures all adsorption sites are fully populated. It was observed that a new high-frequency form of chemisorbed CO, designated CO*, is populated, and that its saturation intensity in the i.r. is proportional roughly to the S coverage. In figure 7, the onset of CO* formation at low S coverages is shown. It should be noted that over the CO* coverage range observed in our work at various S coverages, little shift in frequency from 2108 cm$^{-1}$ is observed. Furthermore, the remaining terminal and bridged-CO species essentially retain their full-coverage frequencies as various coverages of CO* are produced by changing the S coverage. At high coverages, CO* is the only species present, in agreement with Erley & Wagner (1978), who found that at 300 K and in ultra-high vacuum, little CO remains on S/Ni(111) at $\theta_s = 4.4 \times 10^{18}$ S atoms per square metre. Under their conditions of temperature and pressure, CO* would not have been present owing to its low heat of adsorption (Trenary *et al.* 1985).

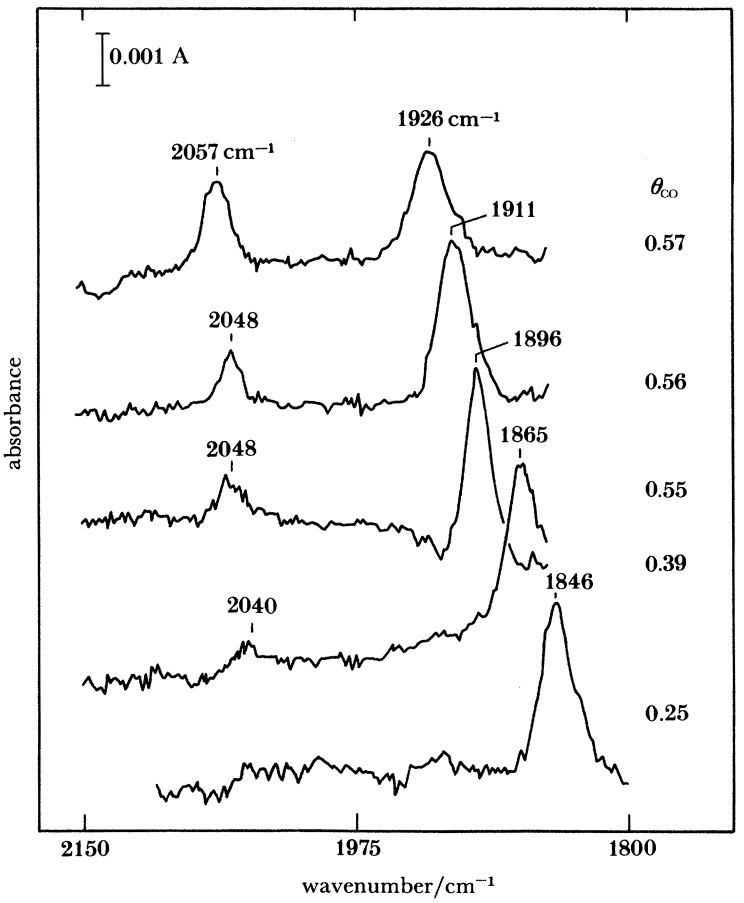


FIGURE 7. Onset of chemisorption of terminal CO on Ni(111) at 80 K.

In an effort to quantitatively determine the heat of adsorption of the CO* state, we have used the integrated intensity of the CO* absorption band as a means of CO* coverage measurement. Relative equilibrium CO* coverages were measured as a function of temperature under a CO pressure of 133 N $m^{-2}$, following the method of Wang & Yates (1984). The spectra and the plot of $\ln K_{eq}$ against $T^{-1}$ are shown in figure 9. The heat of chemisorption of CO* is 79 kJ $mol^{-1}$, compared to 111 kJ $mol^{-1}$ for CO on clean Ni(111) (Christmann *et al.* 1974; Conrad *et al.* 1976). Saturation of CO* sites at 300 K may be achieved at $P_{CO} = 133$ N $m^{-2}$, as shown in figure 10. It should again be noted that large changes in the frequency of CO* do not occur over its total range of coverage.

(ii) *Thermal desorption spectroscopy investigations*

By working at 80 K, it is possible to retain the chemisorbed CO* state in vacuum and hence to use t.d.s. to study CO* saturation surface concentration as a function of S coverage. Characteristic desorption spectra for various S coverages are shown in figure 11, where the hatched area is attributed to CO*, and the non-hatched area is attributed to desorption from sites that are not influenced by S. The non-hatched areas are normalized CO desorption traces from clean Ni(111), fit to the various t.d. spectra from Ni(111) containing various levels of S. Two effects are seen here: (1) the CO* coverage initially increases with increasing S coverage; (2) The total CO coverage decreases with increasing S coverage.

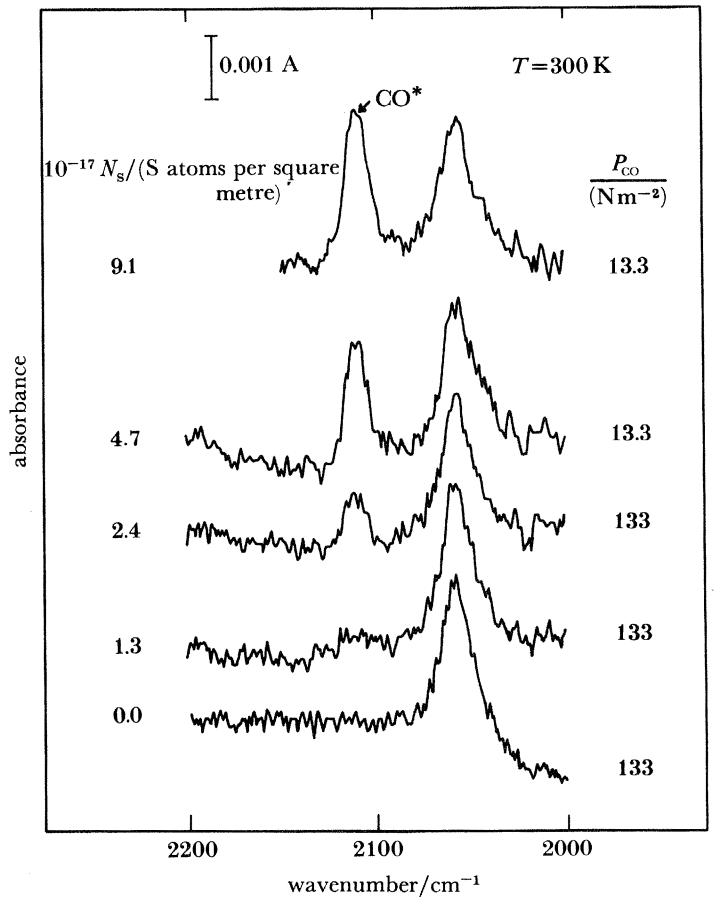


FIGURE 8. Onset of chemisorption of CO* on S-perturbed Ni(111) at high CO pressures.

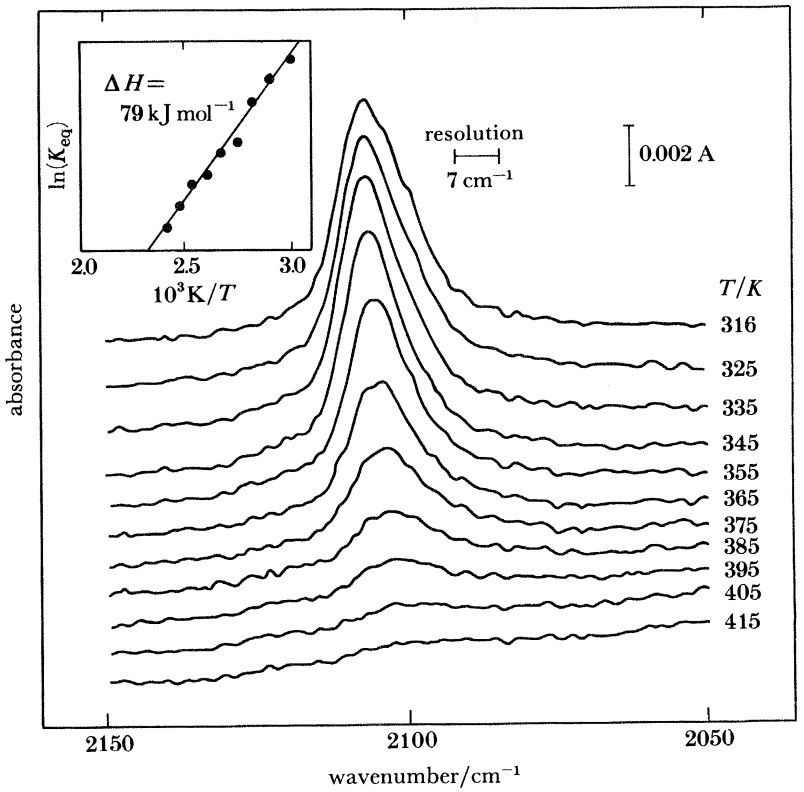


FIGURE 9. Temperature dependence of CO* absorption band. Determination of the heat of chemisorption of CO*; $P_{CO} = 133$ N m$^{-2}$, $N_S = 2.32 \times 10^{18}$ S atoms per square metre.

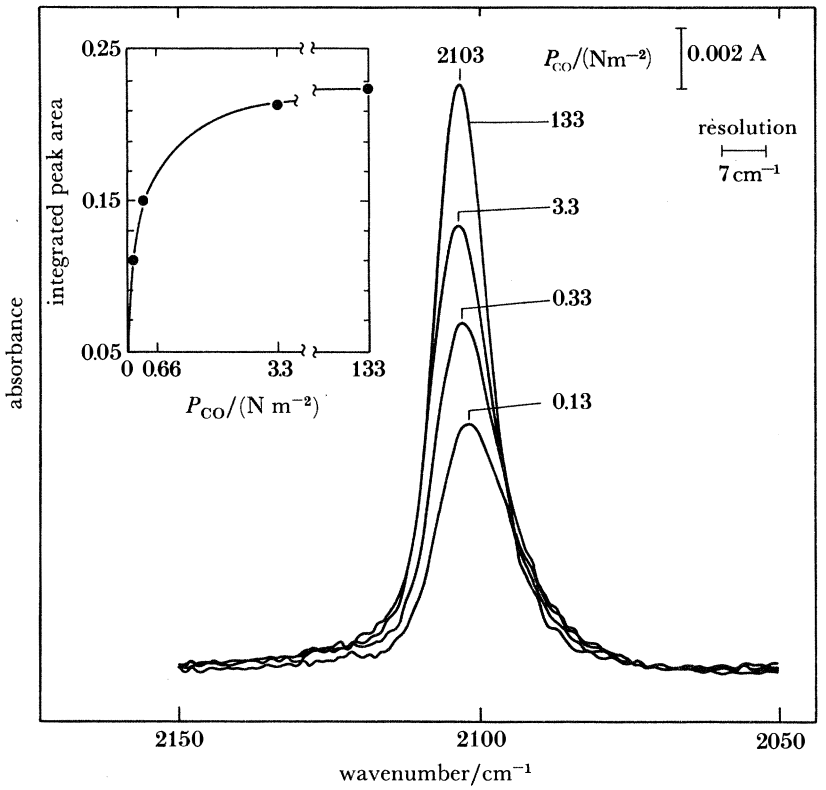


FIGURE 10. Evidence for saturation of S-induced CO* state on Ni(111) at high CO pressure. The S atom coverage, $N_S = 3.3 \times 10^{18}$ m$^{-2}$. The temperature for the inset data is 300 K.

We define the coverage of CO* as $N_{CO*}$, and the coverage of unperturbed CO as $N_{CO}$. The total CO coverage on the sulphided surface is therefore $N_{CO*} + N_{CO}$. Figure 12*a* shows two plots of $N_{CO} + N_{CO*}$ and $N_{CO*}$ against S coverage.

The limiting behaviour of the CO + S interaction at low S coverages may be determined from the initial slopes of the plots in figure 12. When the total coverage of CO is measured (figure 12*a*), it is found that one S atom displaces about 2.1 CO molecules; in addition, one S atom produces about 1.4 CO* species, as shown. Figure 12*b* shows the combination of these two effects, in which, under limiting conditions of low S coverage, 3.5 CO molecules are influenced per S adsorbate. The plot in figure 12*b* is remarkably similar to results of Madix *et al.* (1983*a*, *b*) for S + CO interactions on Ni(100), where 3.5 CO molecules were displaced per S atom at 160 K.

### (*c*) CO *adsorption on* Ni(111) *by surface Penning ionization electron spectroscopy*

The surface Penning ionization electron spectroscopy (s.P.i.e.s.) technique offers a unique sensitivity for examination of the molecular orbitals involved in chemisorption. Because the cross section for excitation of the Penning process is dependent upon overlap of the excited-state atomic orbital of He($2^1$S) with filled adsorbate orbitals, s.P.i.e.s. offers roughly the same information about adsorbed species as ultraviolet photoelectron spectroscopy, with a spatial bias for those orbitals extending outward from the surface.

Figure 13 shows the development of the s.P.i.e.s. spectrum for CO on Ni(111). We see

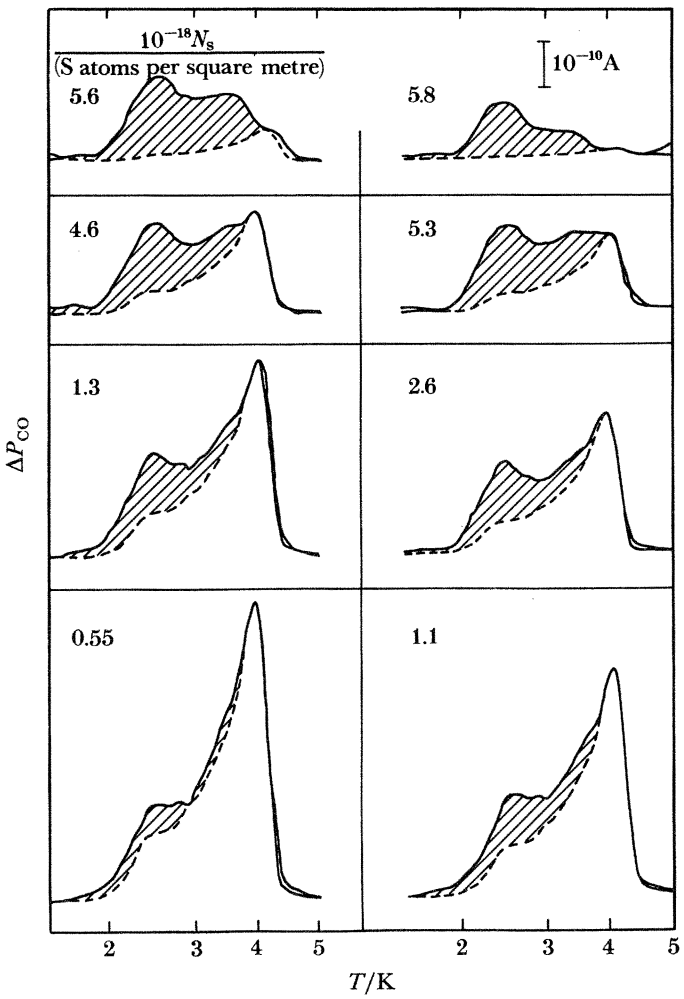


FIGURE 11. Production of new CO desorption states by S on Ni(111): state resolution. Hatched areas are attributed to CO*.

clearly the development of $4\sigma$, $(1\pi+5\sigma)$, and $2\pi^*$ emission from the CO orbitals (Bozso *et al.* 1983). The $2\pi^*$ density of states originates from the interaction of empty CO $2\pi^*$ orbitals with metal electrons. The lowering of the energy of the $2\pi^*$ orbital places part of the density of states below the Fermi energy, causing partial population of this acceptor orbital. This is back-donation, a significant factor in CO chemisorption on transition metals; these data provide direct evidence of CO acceptor behaviour in chemisorption.

## 4. DISCUSSION

### (*a*) CO–CO *interaction on* Ni(111)

The i.r. and l.e.e.d. data shown in figure 5 are indicative of two stable hybridization states for CO chemisorbed on Ni(111) at full CO coverage. These are twofold-bridged and terminally bonded CO (Sheppard & Nguyen 1978). Under conditions of adsorption (80 K) where long-range order does not exist (no l.e.e.d. pattern) these two basic states of CO hybridization

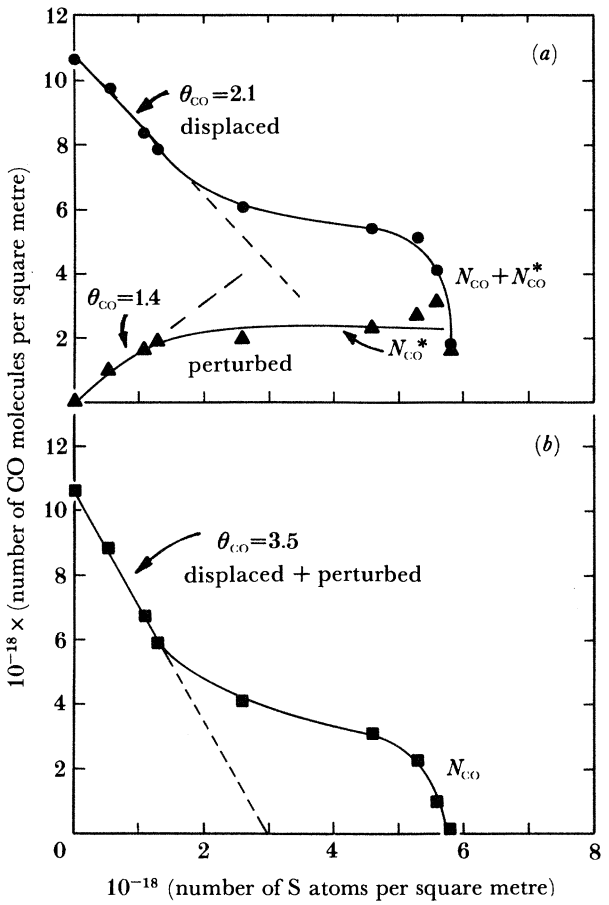


FIGURE 12. Effect of S coverage on the surface coverage of various CO desorption states. The temperature is 85 K.

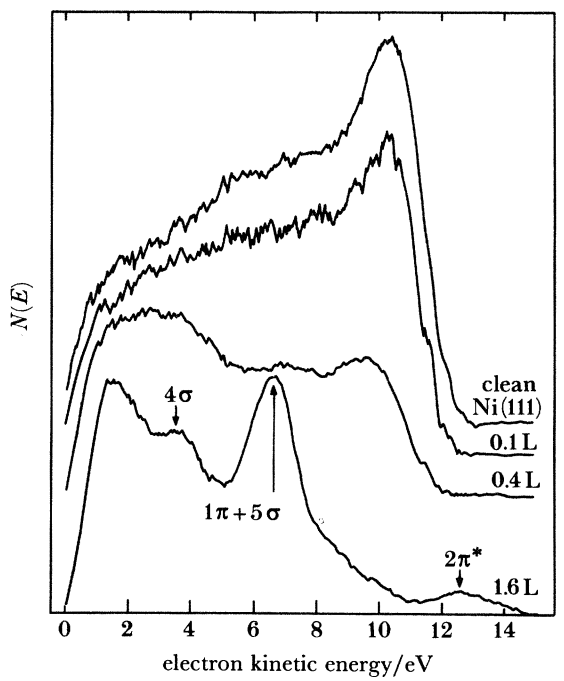


FIGURE 13. Development of s.P.i.e. spectrum for CO on Ni(111) at 290 K by using $2^1$S He as an excitation source. CO exposures given in Langmuir (1 L = $1.33 \times 10^{-4}$ N s m$^{-2}$).

are still observed (figure 5). This observation suggests that long-range ordering of CO species has little to do with the selection of a hybridization state by a given CO molecule; instead, it is competition for metal electrons by an acceptor CO species that determines how it will hybridize. As the coverage of CO increases on Ni(111), back-donation of electrons from the metal becomes less favourable on average, and CO molecules begin to bond in a terminal mode (having lower acceptor character), a phenomenon due to lowered donor capability of the metal. Indeed, in the transformation from $c(4\times2)\rightarrow(\frac{1}{2}\sqrt{7}\times\frac{1}{2}\sqrt{7})$ R 19.1°, bridged-CO molecules are actually consumed as coverage rises to saturation (0.50 bridged-CO/Ni $\rightarrow$ 0.43 bridged-CO/Ni).

In figure 6, where the frequency of bridged CO is plotted against CO coverage, the initial upward shift may be interpreted as being due to a mixture of chemical and electrodynamic effects between CO species (Crossley & King 1977; Bradshaw 1982), although these details have not yet been worked out for this system. Near the coverage where terminal-CO species first begin to populate the Ni(111) surface, a sharp upturn in the frequency of bridged CO is observed. This effect is almost certainly due to the onset of severe competition for back-donating metal electrons, leading to the production of terminal CO having lower acceptor needs. Since the bridged-CO coverage decreases in this particular region, electrodynamic coupling between dynamic dipoles cannot explain the shift.

Similar donor-acceptor ideas have been used to explain the coverage-dependent (and stoichiometric) conversion of bridged-CO to terminal-CO on supported Pd particles by Gelin & Yates (1984*a*, *b*). Here, by using isotopic labelling of preadsorbed bridged CO, it was shown that additional adsorption of unlabelled CO caused significant bridged–terminal conversion at 80 K. A similar picture for CO adsorption on Pt(110) was proposed by Bare *et al.* (1984), although donor–acceptor concepts were not specifically invoked.

We therefore believe that chemical effects involving bonding electron availability in the l.d.o.s. near $E_F$ (a long-range phenomenon) control the hybridization state chosen by a given CO molecule in the chemisorbed layer. This is probably a general concept at work in many chemisorption systems.

### (*b*) CO . . . S *interactions on* Ni(111)

#### (i) *Local electronic effects near chemisorbed S*

In distinct contrast to the coverage-dependent frequency shifting for CO on Ni(111), and to the final development of terminal CO in a field of bridged-CO species, the presence of impurity S on Ni(111) produces a new site capable of adsorbing only one form of terminal CO, designated CO*. This high-frequency CO* species exhibits little shift in frequency at various coverages (figure 9).

The singular character of CO* suggests that it is *locally* associated with an S impurity atom. The work of Feibelman & Hamann (1984) and Norskov *et al.* (1984) would suggest that CO* is bound to a Ni atom in contact with an S atom, and that local electrostatic effects influence the bonding character of CO*, a seen by its high frequency. From figure 1*a* it is seen that S causes an enhanced valance electron charge density in its vicinity above the metal surface. The local induced electric field caused by this charge redistribution will oppose back-donation into the antibonding $2\pi^*$ orbital of CO, causing the CO* frequency to be increased, as is observed. By using s.P.i.e.s. to examine the degree of population of CO $2\pi^*$ when CO interacts with K(ads) on Ni(111), the opposite effect has been seen with $K^{\delta+}$ inducing increased population

of $2\pi^*$ (Lee *et al.* 1983*a*,*b*). Similar studies with electronegative adsorbates and CO have not yet been undertaken.

The lowered binding energy for CO* (79 kJ $mol^{-1}$ cf. 111 kJ $mol^{-1}$ for clean Ni(111)) is also consistent with the Feibelman & Hamann (1984) model, since, as shown in figure 2, the l.d.o.s. at this near-neighbour site will be lowered, leading to a lower metal–CO interaction energy.

Finally, the local interaction between chemisorbed S and CO* is also consistent with the observation by i.r. and by t.d.s. that unperturbed terminal and bridged-CO species persist to high S coverages.

(ii) *Quantitative model for* S *poisoning on* Ni(111)

The quantitative evaluation of the range of influence of an S atom on Ni(111) has been made by using t.d.s. methods in which CO* is initially retained on the S/Ni(111) surface at low temperatures. As shown in figures 11 and 12, S adsorption causes two effects: (1) S adsorption induces CO* sites; ;(2) S adsorption decreases the total saturated coverage of CO.

Figure 12 shows that about 3.5 CO species are influenced by 1 S impurity atom. Since the full CO coverage is 0.57 CO per Ni atom (figure 5), this means that about 6 Ni sites are influenced by a single S atom. The CO* species are *produced* at an initial rate of 1.4 CO* per S atom; CO is displaced at an initial rate of 2.1 CO per S atom.

A model based on the Feibelman & Hamann (1984) picture and consistent with our measurements is shown in figure 14. Here, an S atom in a three-fold Ni(111) hollow site influences three nearest Ni sites to potentially produce three CO* sites designated by an asterisk. On average, about one-half of these are occupied by CO* at full CO* coverage. In this model, the next-nearest neighbour Ni sites, indicated by −, cannot adsorb CO because of unfavourable

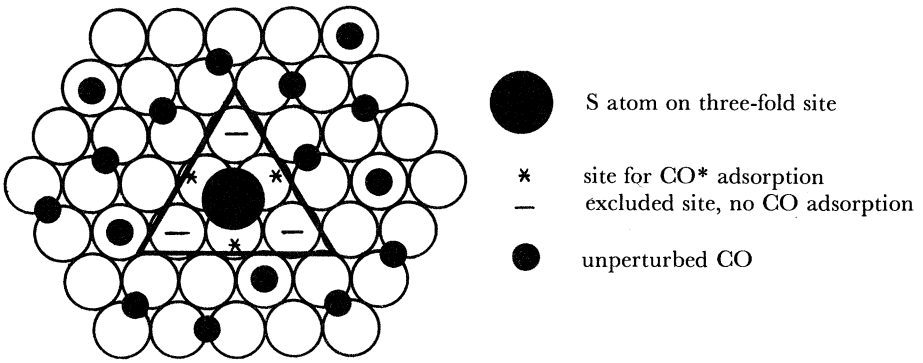


FIGURE 14. Possible S poisoning local model for CO on Ni(111). This model includes the production of a site adjacent to S, labelled with an asterisk, which adsorbs a CO* species. The next nearest-neighbour sites, designated −, are unable to adsorb CO. Unperturbed CO molecules exist in a $(\frac{1}{2}\sqrt{7} \times \frac{1}{2}\sqrt{7})$ R 19.1° structure as shown.

effects of S on the l.d.o.s. at these sites. Beyond the six Ni-atom region, CO exists unperturbed at full coverage.

These results are in general agreement with Gland *et al.* (1984) for CO + S/Ni(100), where a $c(2 \times 2)$ S structure induced a CO* band at 2115 $cm^{-1}$. However, they emphasize local steric effects of S rather than local electrostatic effects. The six Ni-site range of the effect of S on




PHILOSOPHICAL TRANSACTIONS OF THE ROYAL SOCIETY A MATHEMATICAL, PHYSICAL & ENGINEERING SCIENCES

Ni(111) sites is also in good agreement with the work of Goodman & Kiskinova (1981*a*,*b*), who used reaction kinetic measurements to evaluate the effect of poisons on Ni(100), to obtain similar results.

## 5. Summary

The following general concepts have been developed in this work:

(1) Short-range interactions between an electronegative adsorbate and CO occur locally through electrostatic effects, mixed with effects due to changes in the local density of states by the electronegative species.

(2) Long-range adsorbate–adsorbate interactions are primarily related to the perturbation of the local density of states. These interactions may influence adsorbate hybridization states through a donor–acceptor mechanism, as observed for CO.

(3) S poisoning of Ni, as judged by the vibrational behaviour of chemisorbed CO, is composed of a mixture of electrostatic and local density of states factors. A specific high-frequency form of CO having a lowered surface binding energy is produced. This specific type of CO may be bound to nearest-neighbour Ni sites to S. A total of about six Ni sites per S are perturbed for CO adsorption, with three next-nearest neighbours being unable to chemisorb CO.

(4) The influence of electropositive and electronegative impurity atoms can be directly probed with surface Penning ionization electron spectroscopy. S.P.i.e.s. results for CO/K/Ni(111) clearly show an increase in CO + $2\pi^*$ electron density. This result and the CO/S/Ni(111) vibrational data are both explained by the same general mechanism for the interaction of CO with coadsorbed impurity atoms.

We gratefully acknowledge support of the i.r. work by the Department of Energy, Division of Basic Energy Sciences, and support of the s.p.i.e.s. work by the N.S.F.

## References

Bare, S. R., Hofmann, P. & King, D. A 1984 *Surf. Sci.* **144**, 347–369.
Bertolini, J. C., Dolmai-Imelik, G. & Rousseau, J. 1977 *Surf. Sci.* **68**, 539–546.
Bertolini, J. C. & Tardy, B. 1981 *Surf. Sci.* **102**, 131–150.
Bozso, F., Yates, J. T., Jr, Arias, J., Metiu, H. & Martin, R. M. 1983 *J. chem. Phys.* **78**, 4256–4269.
Bradshaw, A. *Appl. surf. Sci.* 1982 **11**, 712–729.
Campuzano, J. C. & Greenler, R. G. 1979 *Surf. Sci.* **83**, 301–312.
Christmann, K., Schober, O. & Ertl, G. 1974 *J. chem. Phys.* **60**, 4719–4724.
Conrad, H., Ertl, G., Küppers, J. & Latta, E. E. 1976 *Surf. Sci.* **57**, 475–484.
Crossley, A. & King, D. A. 1977 *Surf. Sci.* **68**, 528–538.
Erley, W. & Wagner, H. 1978 *J. Catal.* **53**, 287–294.
Erley, W., Wagner, H. & Ibach, H. 1979 *Surf. Sci.* **80**, 612–619.
Feibelman, P. J. & Hamann, D. R 1984 *Phys. Rev. Lett.* **52**, 61–64.
Feibelman, P. J. & Hamann, D. R. 1985 *Surf. Sci.* **149**, 48–66.
Gelin, P., Siedle, A. R. & Yates, J. T. Jr 1984 *J. phys. Chem.* **88**, 2978–2985.
Gelin, P. & Yates, J. T. Jr 1984 *Surf. Sci.* **136**, L1–K8.
Gland, J. L., Madix, R. J., McCabe, R. W. & Demaggio, C. 1984 *Surf. Sci.* **143**, 46–56.
Goodman, D. W. & Kiskinova, M. *Surf. Sci.* 1981*a* **105**, L265–270.
Kiskinova, M. & Goodman, D. W. *Surf. Sci.* 1981*b* **108**, 64–76.
Lee, J., Hanrahan, C. P., Arias, J., Martin, R. & Metiu, H. *Phys. Rev. Lett.* 1983*a* **51**, 1803–1806.
Lee, J., Arias, J., Hanrahan, C. P., Martin, R. & Metiu, H. *Phys. Rev. Lett.* 1983*b* **51**, 1991–1994.
Madix, R. J., Lee, S. B. & Thornburg, M. 1983*a* *Surf. Sci.* **133**, L447–451.
Madix, R. J., Lee, S. B. & Thornburg, M. 1983*b* *J. Vac. Sci. Technol.* A**1**, 1254–1260.


PHILOSOPHICAL TRANSACTIONS OF THE ROYAL SOCIETY A MATHEMATICAL, PHYSICAL & ENGINEERING SCIENCES

Netzer, F. & Madey, T. E. 1982 *J. chem. Phys.* **76**, 710–715.
Norskov, J. K., Holloway, S. & Lang, N. D. 1984 *Surf. Sci.* **137**, 65–78.
Sheppard, N. & Nguyen, T. T. 1978 *Advances in infrared and Raman spectroscopy*, vol. 5, pp. 67–148.
Trenary, M., Uram, K. J. & Yates, J. T. Jr 1985 *Surf. Sci.* **157**, 512–538.
Wang, H. P. & Yates, J. T. Jr 1984 *J. phys. Chem.* **88**, 852–856.

*Discussion*

S. Holloway (*Department of I.P.I. Chemistry, Donnan Laboratories, University of Liverpool, U.K.*). During discussions concerning the effects of co-adsorbed electronegative species on molecular bonding (relating to so-called poison and promotion effects), Professor Yates draw attention to recent SLAPW calculations (Feibelman & Hamann 1984) where the effect of modifications to changes in local densities of states at the $\Delta n(\epsilon_F)$ were presented. Although it is not at all clear how one relates such effects as $\Delta n(\epsilon_F)$ to the changes in total binding energy or indeed inter-molecular vibrational frequencies of species adsorbed in neighbouring sites, it is possible to estimate such changes if one is prepared to forego *ab initio* rigour. It is essential (as was stressed in Feibelman & Hamann 1984) to include a good description of screening at the surface. While the jellium model does not include the effect of a crystal lattice, it does include (self-consistently) metallic screening, and recently the effects of poison (and promotor) – molecule interactions based on such calculations have been presented. Here it was shown that the first-order change in binding energy, $\Delta E$, of a molecule could be expressed as (Norskov *et al.* 1984)

$$\Delta E = \int_a \delta\varphi_0(\boldsymbol{r})\,\Delta p(\boldsymbol{r})\,\mathrm{d}\boldsymbol{r} + \delta\left\{\int_{-\infty}^{\epsilon_F} \epsilon n(\epsilon)\,\mathrm{d}\epsilon\right\},$$

where $\delta\varphi_0(\boldsymbol{r})$ is the self-consistent electrostatic potential around the co-adsorbed poison or promotor species and $\Delta p(\boldsymbol{r})$ is the induced electron density (including nuclei) of the adsorbed molecule. The first term is, in essence, the electrostatic interaction energy between coadsorbates. It has been shown that a detailed examination of this term alone accounts for quite a body of existing experimental data (Lang *et al.* 1985). The second term accounts (in a very crude way), for the electronic interaction between the molecule and the change to the local electronic interaction between the molecule and the change to the local electronic structure from the promotor or poison. It is this second term that could be related to effects discussed in (Feibelman & Hamann 1984). While it would, of course, be of great interest to estimate the size and sign of the change in binding energy arising from this effect, it would be of more direct interest to examine the form of $\delta\varphi_0(\boldsymbol{r})$ for the case of a more realistic surface, as presented in (Feibelman & Hamann 1984) to compare with results for a jellium surface.

*Reference*

Lang, N. D., Holloway, S. & Norskov, J. K. 1985 *Surf. Sci.* **150**, 24.




PHILOSOPHICAL TRANSACTIONS OF THE ROYAL SOCIETY A MATHEMATICAL, PHYSICAL & ENGINEERING SCIENCES